Molecular Recognition of K^+ and Na^+ by Valinomycin in Methanol

Tami J. Marrone and Kenneth M. Merz, Jr.*

Contribution from the Department of Chemistry, The Pennsylvania State University, University Park, Pennsylvania 16802

Received May 5, 1993[⊗]

Abstract: Potential of mean force (PMF), free energy perturbation (FEP), and molecular dynamics (MD) simulations were used to examine the association processes of K^+ and Na^+ with valinomycin in methanol. The estimated absolute free energy of binding of Na^+ to valinomycin is ~1.1 to −2.5 kcal/mol, which is in reasonable agreement with the available experimental value of -1.2 ± 0.4 kcal/mol. The calculated K^+ free energies of association through the preferred HyV (isopropyl) face (the Lac (methyl, isopropyl) face was found to be disfavored) of valinomycin are −7.4 to −12.5 kcal/mol. This range of values overestimates the experimental free energy of binding (-6.4 ± 0.4 kcal/mol) by ~1−6.1 kcal/mol, respectively. Graphical analysis and MD trajectories at various points of the PMF profiles show that the association/dissociation processes of K^+ and Na^+ are qualitatively similar, and the difference in binding affinity is based on the solvation free energy of the ions in methanol.

Introduction

Molecular recognition is of fundamental importance in biochemistry and chemistry.[1-3] Antibiotic ionophores are small biological molecules that recognize ions and transport them across cell membranes.[4-6] These molecules have been studied extensively in an attempt to understand their molecular recognition properties.[4-6] Valinomycin, a naturally occurring ionophore, has long been recognized for its ability to bind K^+ more strongly than Na^+. For example, valinomycin binds K^+ more strongly than Na^+ by ~5 kcal/mol in methanol.[7] This high selectivity is intriguing because the molecule is known to be conformationally flexible in methanol.[5] Synthetic ionophores usually achieve selectivity through rigidity by making the cavity that binds the ion the perfect size for one particular ion.[1] Therefore, valinomycin has the unusual set of combined properties of selectivity and conformational flexibility.

Valinomycin is a member of the depsipeptide family of molecules. It is a cyclic molecule consisting of 12 alternating residues of amino acid and hydroxy acid residues. It has the formula (D-Val-L-Lac-L-Val-D-HyV)$_3$ where Val is valine, Lac is lactic acid, and HyV is hydroxyvaleric acid. The selectivity sequence for the alkali cations is $Rb^+ > K^+ \gg Cs^+ > Na^+ > Li^+$ in methanol.[4] Crystallographic structures for valinomycin have been solved for the uncomplexed form[8-10] as well as several ion-complex forms.[11-13] The crystal structure of the uncomplexed form of valinomycin grown in DMSO[9] (see Figure 1) shows the molecule with a "propeller" shape with three intramolecular hydrogen bonds between the D-Val and L-Lac residues. The crystal structure obtained from crystals grown in octane[10] (Figure 2) shows a very different structure than the structure taken from crystals grown in DMSO. Six intramolecular hydrogen bonds hold the complex together, and the structure is that of a distorted "bracelet" that qualitatively resembles the crystal structure of the potassium complex as described below. NMR studies show the uncomplexed valinomycin molecule to be very conformationally flexible since it exhibits several conformations in different solvents.[14,15] In the crystal structure of the potassium complex[11] (Figure 3), valinomycin forms a cage around the ion that resembles a bracelet. The molecule shows six tight turns held together by intramolecular hydrogen bonds. In this bracelet form, the ion sits in the center of the complex surrounded by hydrophilic groups that line the cage. The ion is coordinated by six carbonyl oxygens from the valine groups. Methyl and isopropyl groups project out of the complex and form the hydrophobic exterior of the cage. This hydrophilic interior with a hydrophobic exterior makes the molecule ideal for transporting an ion across a hydrophobic lipid membrane.

There are two faces of the complexed valinomycin molecule through which the ion can pass during decomplexation; the Lac face and the HyV face. The Lac face contains three methyl groups from the Lac residues and three isopropyl groups from the D-valine residues, while the HyV face contains six isopropyl

[⊗] Abstract published in *Advance ACS Abstracts,* December 15, 1994.

(1) Cram, D. J. The Design of Molecular Hosts, Guests, and Their Complexes. *Science* **1988**, *240*, 760–767.
(2) Lehn, J.-M. Supramolecular Chemistry − Scope and Perspectives: Molecules, Supermolecules, and Molecular Devices. *Angew. Chem., Int. Ed. Engl.* **1988**, *27*, 90–112.
(3) Rebek, J. Model Studies in Molecular Recognition. *Science* **1987**, *235*, 1478–1484.
(4) Dobler, M. *Ionophores and Their Structures*; John Wiley and Sons: New York, 1981.
(5) *Membranes: A Series of Advances*; Eisenman, G., Ed.; Marcel Dekker: New York, 1975; Vol. 3.
(6) Ovchinnikov, Y. A.; Yivanov, V.; Shkrob, A. M. *Membrane Active Complexones*; Elsevier: Amsterdam, 1974.
(7) Izatt, R. M.; Bradshaw, J. S.; Nielson, S. A.; Lamb, J. D.; Christensen, J. J.; Sen, D. Thermodynamic and Kinetic Data for Cation−Macrocycle Interaction. *Chem. Rev.* **1985**, *85*, 271–339.
(8) Smith, G. D.; Daux, W. L.; Langs, D. A.; DeTitta, G. T.; Edmonds, J. W.; Rohrer, D. C.; Weeks, C. M. The Crystal and Molecular Structure of the Triclinic and Monoclinic Forms of Valinomycin, C54H90N6O18. *J. Am. Chem. Soc.* **1975**, *97*, 7242–7247.
(9) Karle, I. L.; Flippen-Anderson, J. L. A New Conformation Exhibiting Near-Threefold Symmetry for Uncomplexed Valinomycin in Crystals from Dimethyl Sulfoxide. *J. Am. Chem. Soc.* **1988**, *110*, 3253–3257.
(10) Karle, I. Conformation of Valinomycin in a Triclinic Crystal Form. *J. Am. Chem. Soc.* **1975**, *97*, 4379–4386.
(11) Neupert-Laves, K.; Dobler, M. The Crystal Structure of a K+ Complex of Valinomycin. *Helv. Chim. Acta* **1975**, *58*, 432–442.
(12) Hamilton, J. A.; Sabesan, M. N.; Steinrauf, L. K. Crystal Structure of Valinomycin Potassium Picrate Anion Effects on Valinomycin Cation Complexes. *J. Am. Chem. Soc.* **1981**, *103*, 5880–5885.
(13) Devarajan, S.; Nair, C. M. K.; Easwaran, K. R. K.; Vijayan, M. A Novel Conformation of Valinomycin in its Barium Complex. *Nature* **1980**, *286*, 640–641.
(14) Patel, D. J.; Tonelli, A. E. Solvent−Dependent Conformations of Valinomycin in Solution. *Biochemistry* **1973**, *12*, 486–501.
(15) Tabeta, R.; Saitô, H. High-Resolution Solid State 13C NMR Study of Free and Metal-Complexed Macrocyclic Antibiotic Ionophores Valinomycin, Nonactin, and Tetranactin: Conformational Elucidation in Solid and Solution by Conformation-Dependent 13C Chemical Shifts. *Biochemistry* **1985**, *24*, 7696–7702.

0002-7863/95/1517-0779$09.00/0 © 1995 American Chemical Society

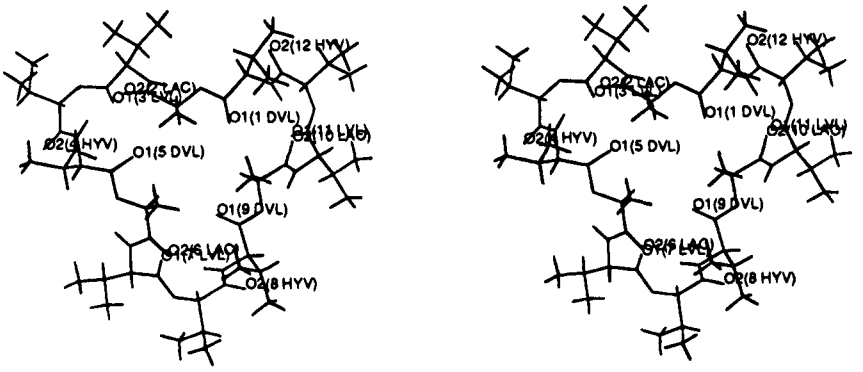

Figure 1. Stereoview of the uncomplexed valinomycin crystal structure. The crystals were grown in DMSO.

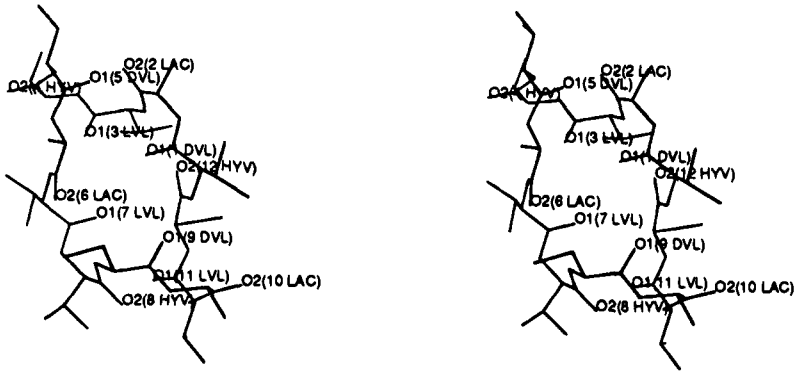

Figure 2. Stereoview of the uncomplexed valinomycin crystal structure. The crystals were grown in octane.

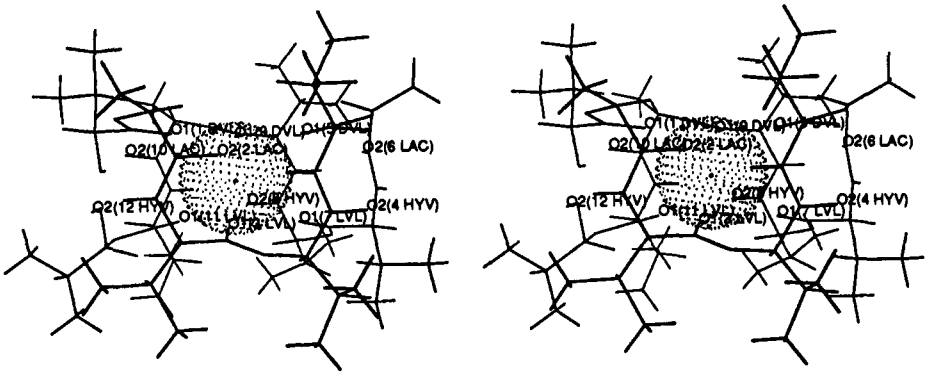

Figure 3. Stereoview of the crystal structure of valinomycin complexed with K^+. The top face of the molecule is the Lac face while the bottom face is the HyV face.

groups from three HyV residues and three L-valines. This makes the HyV face more hydrophobic than the Lac face.

Previously, gas phase theoretical studies have been done to try to understand the selectivity of the valinomycin molecule.[16-19] Recently, Åqvist and co-workers studied the selectivity in methanol using free energy perturbation techniques[20] and showed that the Lac face is prone to methanol attack. Although free energy perturbation calculations can predict selectivities, they cannot verify if a particular potential function representation is accurate. Furthermore, they cannot describe the ion dissociation or association pathway into the complex. Potential of mean force (PMF) simulations have been successful in providing insights into ionophore–ion complexation processes.[21-23] PMF calculations accumulate the free energy as a function of distance as the ion is pulled out of the complex. Analysis of the selected reaction profile provides energetic and structural information about the association/dissociation process. Molecular dynamics (MD) trajectories at points along the profile provide structural information about the process. We describe herein PMF simulation results used to describe the association/dissociation

(16) Masut, R. A.; Kushick, J. N. The Molecular Mechanics of Valinomycin. II: Comparative Studies of Alkali Ion Binding. *J. Comput. Chem.* **1985**, *6*, 148–155.

(17) Lifson, S.; Felder, C. E.; Shanzer, A. Enniatin B and Valinomycin as Ion Carriers: An Empirical Force Field Analysis. *J. Biomol. Struct. Dyn.* **1984**, *2*, 641–661.

(18) Pullman, A. Contribution of Theoretical Chemistry to the Study of Ion Transport Through Membranes. *Chem. Rev.* **1991**, *91*, 793.

(19) Eisenman, G.; Åqvist, J.; Alvarez, O. Free Energies Underlying Binding and Transport in Protein Channels: Free Energy Perturbation Simulations of Ion Binding and Selectivity for Valinomycin. *J. Chem. Soc., Faraday Trans.* **1991**, *87*, 2099–2109.

(20) Åqvist, J.; Alvarez, O.; Eisenman, G. Ion-Selective Properties of a Small Ionophore in Methanol Studied by Free Energy Perturbation Simulations. *J. Phys. Chem.* **1992**, *96*, 10019–10025.

(21) van Eerden, J.; Briels, W. J.; Harkema, S.; Feil, D. Potential of Mean Force by Thermodynamic Integration: Molecular-Dynamics Simulation of Decomplexation. *Chem. Phys. Lett.* **1989**, *164*, 370–376.

(22) Dang, L. X.; Kollman, P. A. Free Energy of Association of the 18-Crown-6:K+ Complex in Water: A Molecular Dynamics Simulation. *J. Am. Chem. Soc.* **1990**, *112*, 5716–5720.

(23) Marrone, T. J.; Merz, K. M., Jr. Molecular Recognition of Potassium Ion by the Naturally Occurring Ionophore Nonactin. *J. Am. Chem. Soc.* **1992**, *114*, 7542.

Scheme 1. Thermodynamic Cycle

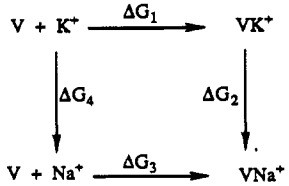

process of K^+ and Na^+ with valinomycin in methanol. We compare the dissociation processes through the Lac face and the HyV face and analyze the differences in association of the K^+ ion and the Na^+ ion.

Theoretical Background

FEP[24-28] simulations have been used to calculate the difference between the free energy of binding of potassium *vs* sodium to valinomycin *via* the thermodynamic cycle shown in Scheme 1. Given that free energy is a state function, the sum of the individual ΔG's of a cycle is zero. For the cycle given in Scheme 1, eq 1 shows the free energy relationship. Rearrangement of eq 1 to solve for the relative free energy of binding results in eq 2. In these simulations the potassium ion is slowly perturbed to the sodium ion in solution (ΔG_4) and in the valinomycin complex (ΔG_2). The values obtained this way are then used to calculate the relative free energies of binding of the two ions. FEP simulations accumulate the free energy change as one state is slowly perturbed into another state. In the "slow growth" method, which we have employed here, the perturbation occurs over a period of time via a coupling parameter, λ. A λ value of 1 represents the initial state, and a λ value of 0 represents the final perturbed state. λ is slowly perturbed from 1 to 0, and the free energy change associated with the perturbation is determined from eq 3. V is the potential energy at a particular λ value. The change in potential energy is accumulated over every MD step where n is the total number of MD steps.

$$\Delta G_1 + \Delta G_2 - \Delta G_3 - \Delta G_4 = 0 \tag{1}$$

$$\Delta G_1 - \Delta G_3 = \Delta G_4 - \Delta G_2 = \Delta\Delta G_{\text{bind}} \tag{2}$$

$$\Delta G = \sum_n [V(\lambda + \Delta\lambda) - V(\lambda)]_\lambda \tag{3}$$

The PMF[29-34] is determined using a free energy technique that determines the free energy change along a reaction coordinate. In our work, the PMF is accumulated as a function of the distance between the center of mass (COM) of the ion and the ionophore. The ion is pulled out of the ionophore stepwise in a series of windows to obtain a free energy profile that can then be used to obtain an association constant. The association constant for the process is calculated *via* eq 4.[35] K_a is the association constant, $W(r)$ is the potential of mean force, k is Boltzman's constant, T is temperature, N is Avogadro's number, and r_c is the cutoff distance for association. In this method, the two species that are associating are assumed to be spherical in shape, but in the case of valinomycin associating with an ion, this is a relatively poor approximation. To improve the situation slightly, we have modified this approach by assuming that the target area for association of the spherical ion is a hemisphere (*i.e.*, valinomycin); however, this approach should still be viewed as an approximation as should the association constants determined in this manner. The association constant is then used to calculate the free energy of binding through eq 5, where ΔG is the absolute free energy of binding.

$$K_a = N\int_0^{r_c} 4\pi r^2 \exp[-W(r)/kT]\, dr \tag{4}$$

$$\Delta G = -RT \ln K_a \tag{5}$$

A second procedure is to use the free energy profile to determine k_{on} and k_{off} and hence, K_a. This method (as well as the previous one) is sensitive to the shape of the free energy profile and again should be viewed as an estimate of the "true" K_a. In the present paper both of these methods have been used to obtain a range of values possible for the absolute free energy of binding of ions to valinomycin.

In what follows, we will discuss the parameterization procedure used to obtain a charge model for valinomycin, the FEP results used to test the charge models, the results of the PMF simulations, and the results of the MD simulations done at interesting points along the reaction profile, which are aimed at giving us molecular-level insights into the ion association process of valinomycin.

Parameterization

First, we developed force field parameters to describe valinomycin. We parameterized the all-atom AMBER force field,[36] which has the form given in eq 6. The first three terms represent the "bonded"

$$E_{\text{total}} = \sum_{\text{bonds}} K_r/2(r - r_{\text{eq}})^2 + \sum_{\text{angles}} K_\theta/2(\theta - \theta_{\text{eq}})^2 + \sum_{\text{dihedrals}}\sum_n V_n/2[1 + \cos(n\phi - \gamma)] + \sum_{i<j} \epsilon_{ij}\left[\left(\frac{R_{ij}^*}{R_{ij}}\right)^{12} - 2\left(\frac{R_{ij}^*}{R_{ij}}\right)^6\right] + \frac{1}{\text{VDW}_{\text{scale}}}\sum_{\substack{i<j \\ 1-4\text{ terms}}} \epsilon_{ij}\left[\left(\frac{R_{ij}^*}{R_{ij}}\right)^{12} - 2\left(\frac{R_{ij}^*}{R_{ij}}\right)^6\right] + \sum_{\text{H-bonds}}\left[\frac{C_{ij}}{R_{ij}^{12}} - \frac{D_{ij}}{R_{ij}^{10}}\right] + \sum_{i<j}\frac{q_i q_i}{\epsilon R_{ij}} + \frac{1}{\text{EE}_{\text{scale}}}\sum_{\substack{i<j \\ 1,4\text{ terms}}} \frac{q_i q_j}{\epsilon R_{ij}} \tag{6}$$

(24) Zwanzig, R. W. High-Temperature Equation of State by a Perturbation Method. I. Nonpolar Gases. *J. Chem. Phys.* **1954**, *22*, 1420.
(25) van Gunsteren, W. F. The Role of Computer Simulation Techniques in Protein Engineering. *Protein Eng.* **1988**, *2*, 5–13.
(26) Mezei, M.; Beveridge, D. L. Free Energy Simulations. *Ann. N.Y. Acad. Sci.* **1986**, *482*, 1–23.
(27) Jorgensen, W. L. Free Energy Calculations: A Breakthrough for Modeling Organic Chemistry in Solution. *Acc. Chem. Res.* **1989**, *22*, 184–189.
(28) Straatsma, T. P.; McCammon, J. A. Computational Alchemy. *Annu. Rev. Phys. Chem.* **1992**, *43*, 407–435.
(29) Patey, G. N.; Valleau, J. P. A Monte Carlo Method for Obtaining the Interionic Potential of Mean Force in Ionic Solution. *J. Chem. Phys.* **1975**, *63*, 2334–2339.
(30) Bader, J. S.; Chandler, D. Computer Simulation of the Mean Forces between Ferrous and Ferric Ions in Water. *J. Phys. Chem.* **1992**, *96*, 6423–6427.
(31) Buckner, J. K.; Jorgensen, W. L. Energetics and Hydration of the Constituent Ion Pairs in Tetramethylammonium Chloride. *J. Am. Chem. Soc.* **1989**, *111*, 2507–2516.
(32) Dang, L. X.; Pettit, B. M. A Theoretical Study of Like Ion Paris in Solution. *J. Phys. Chem.* **1990**, *94*, 4303–4308.
(33) Elber, R. Calculation of the Potential of Mean Force Using Molecular Dyanmics with Linear Constraints: An Application to a Conformational Transition in a Solvated Peptide. *J. Chem. Phys.* **1990**, *93*, 4312–4321.
(34) Pettit, B. M.; Karplus, M. The Potential of Mean Force Between Polyatomic Molecules in Polar Molecular Solvents. *J. Chem. Phys.* **1985**, *83*, 781–789.
(35) Prue, J. E. Ion Pairs and Complexes: Free, Energies, Enthalpies, and Entropies. *J. Chem. Educ.* **1969**, *46*, 12–16.
(36) Weiner, S. J.; Kollman, P. A.; Nguyen, D. T.; Case, D. A. An All Atom Force Field for Simulations of Proteins and Nucleic Acids. *J. Comput. Chem.* **1986**, *7*, 230–252.

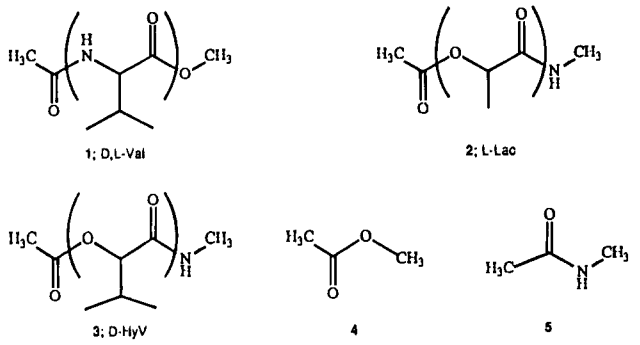

Figure 4. Residues used in the ESP fitting procedure.

interactions present in a molecule, namely the bond, angle, and torsion interactions. The bond angle interactions are represented by a quadratic potential, while the torsional interactions are represented by a truncated Fourier Series. K_x (where $X = r, \theta$) is the force constant for the bond or angle, and X_{eq} is the experimentally observed equilibrium bond length or angle associated with force constant K_x. X is the calculated value for the bond or angle. V_n, n, ϕ, and γ represent the torsional barrier, the periodicity, the calculated dihedral angle, and, finally, the phase. The next five terms represent the "nonbonded" interactions in a molecule. These are the Lennard-Jones (the $R_{ij}^{-12}-R_{ij}^{-6}$ or 6−12 terms), the hydrogen bond (the 10−12 term), and the electrostatic interactions. R_{ij} is the distance between atoms i and j, ϵ_{ij}, R_{ij}^*, C_{ij}, and D_{ij} are parameters that define the shape of the Lennard-Jones potential for the interaction between atoms i and j, q_i and q_j are the atomic point charges for atoms i and j, and ϵ is the dielectric constant.

We derived several atomic point charge models for valinomycin and tested the validity of these models with FEP simulations to determine the set that reproduced experimental data. The first charge model consisted of atom-based point charges derived for each repeating residue present in valinomycin. Gaussian 88[37] was used to carry out electrostatic potential fit (ESP) calculations using the 6-31G* basis set.[38] The *ab initio* ESPs[39-41] were calculated for residues **1**−**3** in Figure 4. To extract the ESP-derived point charges for this residue, we constrained the charges for the atoms outside the parentheses at the values obtained for the ESP-derived charges of **4** or **5**. This maintains the charge neutrality of valinomycin by forcing each residue to be neutral and allows each residue to feel its nearest bonded neighbors.

Two other charge models were obtained by evaluating ESP charges for the whole valinomycin molecule rather than for each residue. In this case, the entire molecule is treated as one residue. The ESP-derived charges were calculated using the MNDO Hamiltonian in the program MOPAC 6.0.[42] Charges were evaluated for both the uncomplexed crystal structure of valinomycin (propeller)[9] and the crystal structure of the potassium complex[11] without the ion (bracelet). The atomic point charges derived for the bracelet structure were used to generate a "classical" (*i.e.*, *via* ESP $= \sum_j q_i q_j / r_{ij}$, where q_i, the probe point, has a charge of +1) ESP surface, which was compared to the quantum mechanically derived ESP surface of the propeller. The same procedure was used to compare the classical-based ESP of the propeller to the quantum mechanically derived ESP of the bracelet. Although each point charge model poorly reproduced the quantum mechanically derived ESP surface of the other structure, the propeller charges better represented the ESP surface of both structures. Thus, we chose to test the propeller charges as a possible charge model for the valinomycin molecule since it better reproduced the charge distribution of two points on the valinomycin potential energy surface. Obtaining a charge model that represents all points along a reaction profile is a challenging problem. One way to solve this is to determine a new charge distribution at every point along a reaction profile, but this is an expensive procedure and is also subject to difficulties arising from conformational flexibility (*i.e.* the charges are sensitive to the instantaneous conformation at which the charges are determined).[43] Ideally, this difficulty could be solved by calculating a charge distribution at every step along an MD trajectory using, for example, a coupled potential method, but currently this is a very expensive proposition. The final charges were symmetrized as appropriate to ensure that symmetry-related groups had identical charges. These charges are found in Tables 1−4 along with the 6-31G*-residue-based charges.

For the present work, bond, angle, torsion, and Lennard-Jones 6−12 parameters and hydrogen bond 10−12 parameters were taken directly from AMBER.[44] The final charge model chosen to represent valinomycin will be discussed in the Results section. The ion parameterization procedure and parameters are described elsewhere.[43]

Table 1. D-Val Charges Obtained from MNDO ESP of Propeller Crystal Structure and a 6-31G*-Residue-Based Approach

	all D-Val residues	
atom	MNDO ESP	6-31G* ESP
N1,3,5	−0.3644	−0.9577
H1,31,61	0.2739	0.4632
C1,19,37	−0.1572	−0.2654
H2,32,62	0.1206	0.1495
C2,20,38	0.2155	0.4865
H3,33,63	−0.0302	−0.0127
C3,21,39	−0.1086	−0.5608
H4,34,64	0.0259	0.1382
H5,35,65	0.0259	0.1382
H6,36,66	0.0259	0.1382
C4,22,40	−0.1086	−0.5608
H7,37,67	0.0289	0.1382
H8,38,68	0.0289	0.1382
H9,39,69	0.0289	0.1382
C5,23,41	0.6344	1.1209
O1,7,13	−0.4421	−0.6919

Table 2. L-Lac Charges Obtained from MNDO ESP of Propeller Crystal Structure and a 6-31G*-Residue-Based-Approach

	all L-Lac residues	
atom	MNDO ESP	6-31G* ESP
O2,8,14	−0.4274	−0.6007
C6,24,42	0.2055	0.4149
H10,40,70	0.0381	0.0925
C7,25,43	0.0068	−0.2986
H11,41,71	0.0004	0.0999
H12,42,72	0.0004	0.0999
H13,43,73	0.0004	0.0999
C8,26,44	0.6052	0.7279
O3,9,15	−0.4841	−0.6357

Simulation Protocols

Free Energy Perturbations. The FEP simulations were done in methanol using the "slow growth" methodology. Constant pressure (1 atm) and constant temperature (298 K) dynamics were used.[45] SHAKE[46] was used to remove the high-frequency motions by restraining bonds to their equilibrium

(37) Frisch, M. J.; Head-Gordon, M.; Schlegel, H. B.; Raghavachari, K.; Binkley, J. S.; Gonzalez, C.; Defrees, D. J.; Fox, D. J.; Whiteside, R. A.; Seeger, R.; Melius, C. F.; Baker, J.; Martin, R.; Kahn, L. R.; Stewart, J. j. P.; Fluder, E. M.; Topiol, S.; Pople, J. A. Available from Gaussian, Inc., Pittsburgh, PA, 1988.

(38) Hehre, W. J.; Radom, L.; van Schleyer, P. R.; Pople, J. A. *Ab Initio Molecular Orbital Theory*; John Wiley: New York, 1986.

(39) Chirlian, L. E.; Francl, M. M. Atomic Charges Derived from Electrostatic Potentials: A Detailed Study. *J. Comput. Chem.* **1987**, *8*, 894−905.

(40) Singh, U. C.; Kollman, P. A. *J. Comput. Chem.* **1984**, *5*, 129.

(41) Williams, D. E.; Yan, J. M. Point-Charge Models for Molecules Derived from Least-Squares Fitting of the Electric Potential. *Adv. At. Mol. Phys.* **1988**, *23*, 87−130.

(42) Stewart, J. J. P. *QCPE Mopac 6.0.*

(43) Marrone, T. J.; Merz, K. M., Jr. Determination of Atomic Charges Including Solvation and Conformational Effects. *J. Phys. Chem.* **1994**, *98*, 1341−1343.

(44) Singh, U. C.; Weiner, P. K.; Caldwell, J.; Kollman, P. A. Available from University of California, San Francisco, 1986.

(45) Berendsen, H. J. C.; Potsma, J. P. M.; van Gunsteren, W. F.; DiNola, A. D.; Haak, J. R. Molecular Dynamics with Coupling to an External Bath. *J. Chem. Phys.* **1984**, *81*, 3684−3690.

Table 3. L-Val Charges Obtained from MNDO ESP of Propeller Crystal Structure and a 6-31G*-Residue-Based Approach

	all L-Val residues	
atom	MNDO ESP	6-31G* ESP
N2,4,6	−0.6945	−0.9577
H14,44,74	0.3582	0.4632
C9,27,45	0.0665	−0.2654
H15,45,75	0.0637	0.1495
C10,28,46	0.2488	0.4865
H16,46,76	−0.0352	−0.0127
C11,29,47	−0.1607	−0.5608
H17,47,77	0.0354	0.1382
H18,48,78	0.0354	0.1382
H19,49,79	0.0354	0.1382
C12,30,48	−0.1607	−0.5608
H20,50,80	0.0354	0.1382
H21,51,81	0.0354	0.1382
H22,52,82	0.0354	0.1382
C13,31,49	0.5480	1.1209
O4,10,16	−0.4024	−0.6919

Table 4. D-HyV Charges Obtained from MNDO ESP of Propeller Crystal Structure and a 6-31G*-Residue-Based Approach

	all D-HyV residues	
atom	MNDO ESP	6-31G* ESP
O5,11,17	−0.3222	−0.4083
C14,32,50	−0.1554	−0.1986
H23,53,83	0.1098	0.1565
C15,33,51	0.2280	0.8205
H24,54,84	−0.0074	−0.2108
C16,34,52	−0.0605	−0.3268
H25,55,85	0.0092	0.0460
H26,56,86	0.0092	0.0460
H27,57,87	0.0092	0.0460
C17,35,53	−0.0605	−0.3268
H28,58,88	0.0092	0.0460
H29,59,89	0.0092	0.0460
H30,60,90	0.0092	0.0460
C18,36,54	0.5023	0.9594
O6,12,18	−0.4674	−0.7411

distances in conjunction with a 1.5 fs time step. The nonbond cutoff was 10 Å, and the nonbond pair list was updated every 25 MD steps. All simulations were done with the AMBER 3A[47] suite of programs and used 615 Jorgensen methanol molecules[48] as the solvent. Due to the incompatible mixing rules between AMBER (additive mixing rule) and OPLS (multiplicative mixing rule) for R*, the minimum for the C- - -O Lennard-Jones interaction is shifted by 0.02 Å, and the repulsive and attractive parts of the potential function differ by 6% and 3%, respectively. From test runs, this resulted in small differences in the MeOH model (note that the C- - -C and O- - -O Lennard-Jones terms are not affected by choice of mixing rule), so we made no modifications to the OPLS MeOH model to account for differences in the mixing rule. Other strategies have been suggested to overcome this problem but were not used by us.[49]

PMF and MD. The PMF and the MD simulations were done at constant volume (box dimensions 38.4 Å × 38.5 Å × 35.1 Å) and constant temperature (298 K). SHAKE was used with a 1.5 fs time step. The nonbond cutoff was 9 Å for the PMF simulations and 10 Å for the MD trajectories. The nonbond pair list was updated every 25 steps. The starting structure for the potassium PMF profiles was an MD-equilibrated crystal structure. The crystal structure was minimized in a box of 615 methanol molecules to remove bad contacts. The ion was then moved to 0 Å separation between the COM of valinomycin and K^+ and heated to 300 K over 400 steps. This point and subsequent points were equilibrated for 9 ps and sampled for 18 ps. The K^+ simulations were performed for 0−9 Å COM separation for both faces, while the Na^+ simulations were performed from 0−9 Å for the HyV face only. The COM separation was incremented by 0.125 Å in the $+z$ direction with respect to the crystal structure coordinates for simulations of ion dissociation through the HyV face. The COM separation was incremented by 0.125 Å in the $-z$ direction with respect to the crystal structure coordinates for simulations of ion dissociation through the Lac face. In order to generate the PMF profile, the COM translational and rotational motion of the ion and valinomycin was removed every MD step.[22,23] The starting structure for the Na^+ PMF profile was created by equilibrating the starting coordinates for the K^+ PMF simulation with Na^+ parameters for 27 ps. Since each COM separation was simulated for 27 ps, the entire association process (0−9 Å) was simulated for 1.97 ns through each face. The MD trajectories at interesting points on the PMF profiles were equilibrated for 27 ps and sampled for 90 ps. Coordinates were collected every 37.5 fs during the sampling phase of the MD trajectory.

Table 5. FEP Results for $VK^+ \rightarrow VNa^+$

charge model	90 ps (kcal/mol)	$\Delta\Delta G_{bind}$ (kcal/mol)[a,b]
6-31G*	unstable	
MNDO	−12.9 ± 1.1	−4.5 ± 1.1

[a] ΔG for $K^+ \rightarrow Na^+$ in MeOH was previously determined as 17.4 ± 0.2 (see ref 44). [b] $\Delta\Delta G_{exp} = -5.2 \pm 0.6$ kcal/mol (averaged from ref 7).

Results

FEP Results. Table 5 contains the results of the FEP simulations of different charge models for the perturbation of the valinomycin K^+ complex to the Na^+ complex. Examination of the results shows that the 6-31G*-residue-based model is unstable over short periods of time and is not a suitable charge model for valinomycin. The charge model obtained from the ESP of the propeller using MNDO[50] holds up over long periods of time, and the relative free energies of binding match well with experimental data. Moreover, calculation of preliminary PMF profiles that used the 6-31G*-residue-based approach gave poor results. On the basis of preliminary PMF results and the relative FEP results, we chose the unscaled propeller charges as the charge model to represent valinomycin in the subsequent PMF simulations. We feel the 6-31G* charge model failed in this instance due to an imbalance between the carbonyl intramolecular hydrogen bonding interactions and carbonyl ion interactions. This causes the carbonyl groups that should be involved in intramolecular hydrogen bonding to become partially coordinated to the ion contained within the cavity of the ionophore. Thus, the bracelet form of complexed valinomycin is unstable relative to a structure in which many of the intramolecular hydrogen bonds are disrupted. Apparently, MNDO ESP charges give a better accounting of these interac-

(46) Ryckaert, J. P.; Ciccotti, G.; Berendsen, H. J. C. Numerical Integration of the Cartesian Equations of Motion of a System with Constraints: Molecular Dynamics of N-Alkanes. *J. Comput. Phys.* **1977**, *23*, 327−341.

(47) Singh, U. C.; Weiner, P. K.; Caldwell, J. W.; Kollman, P. A. *AMBER(UCSF), Version 3.0.*, Revision A; by G. Seibel. AMBER.

(48) Jorgensen, W. L. Optimized Intermolecular Potential Functions for Liquid Alcohols. *J. Phys. Chem.* **1986**, *90*, 1276−1284.

(49) Thomas, B. E., IV; Kollman, P. A. Free Energy Perturbation Calculations of the Relative Binding Affinities of an 8-Subunit Cavitand for Alkali Ions in Methanol. *J. Am. Chem. Soc.* **1994**, *116*, 3449−3452.

(50) Merz, K. M., Jr. Analysis of a Large Database of Electrostatic Potential Derived Atomic Point Charges. *J. Comput. Chem.* **1992**, *13*, 749−767.

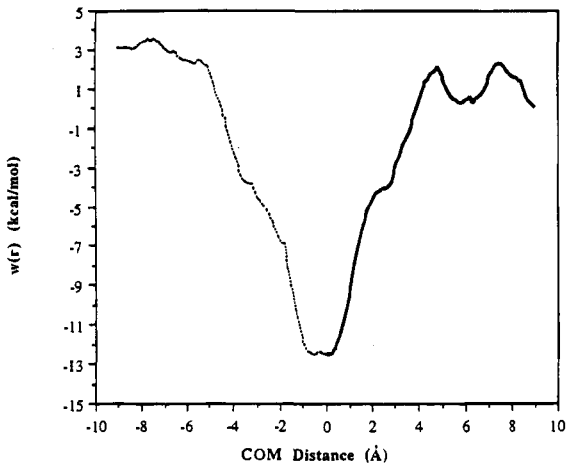

Figure 5. PMF profile for K^+ being discharged through the HyV face (solid line) and the Lac face (dashed line).

tions. An alternative charge model for valinomycin has been reported,[20] but we have not examined this charge set since it was reported after much of this work was completed.

Convergence Results. Before presenting the individual PMF profile results, we need to discuss the error of each individual run used to build up the profile. Propagation of these errors is used to determine the error in the PMF profiles themselves and in the integration of the profiles. Convergence tests were done to determine the error at several points on the K^+ PMF profile and were used to estimate the error in the K^+ and Na^+ PMF curves. Although the error in the two curves is not expected to be identical, the error in the K^+ curve can be used as an estimate of the error in the Na^+ curve.

The standard deviation of five separate runs was determined for six points on the PMF profile: 0.0, 2.0, 4.0, 6.0, 8.0, and 9.0 Å. Each run was equilibrated for 9 ps and sampled for 18 ps. The calculated standard deviations were 0.11, 0.04, 0.03, 0.05, 0.07, and 0.03 kcal/mol, respectively. Using the standard deviation of 0.03 kcal/mol as the lower bound and 0.11 kcal/mol as the upper bound on the error per point, we estimate the error in the curves to be on the order of 0.4−1.3 kcal/mol.

K^+ Results. Figure 5 shows the PMF profiles for K^+ being pulled through the HyV (6 isopropyl) face and the Lac (3 isopropyl, 3 methyl) face of the valinomycin molecule. The HyV profile is represented by the solid line, while the Lac profile is represented by the dashed line. The shapes of the PMF profiles are similar for the Lac and HyV face. Both curves rise steeply in energy until ~2 Å COM separation where there is a slight shoulder. The energy continues to rise until the ion and the valinomycin molecule share a solvent layer (*i.e.*, solvent-separated). Then the energy decreases as the ion and valinomycin become further separated by solvent. We examined the endpoints of the HyV and Lac face simulations graphically. These endopoints are Figures 6 and 7, respectively. Both endpoints are conformationally flexible, and the Lac face structure closely resembles the uncomplexed crystal structure obtained from crystals grown in octane rather than the propeller structure obtained from crystals grown in DMSO. The HyV endpoint, on the other hand, is disordered and is more propeller-like than it is bracelet-like. We chose only to examine the HyV association/dissociation process in detail through MD analysis because it incorporates all the essential features of the molecular recognition. Integration of the HyV profile from 0 to 4.75 Å COM (the maximum) gives the ΔG_{bind} as −7.4 kcal/mol, and a similar integration of the Lac profile gives ΔG_{bind} as −11.5 kcal/mol. These are approximately 1 and 5 kcal/mol higher than the experimental value of −6.4 kcal/mol.

Table 6. Analysis of Percentage of Time the Intramolecular Hydrogen Bonds Exist at Various Points on the K^+ PMF Profile through the HyV Face and the Lac Face Minimum

	percentage of time H-bonded (%)					
H bond	minimum (0.25 Å)	Lac face minimum	2.5 Å	maximum (4.75 Å)	6.25 Å	9.0 Å
N1−H1···O15	87.4	93.1	94.5	80.5	79.9	0.0
N3−H31···O3	97.5	85.6	97.5	0.0	72.9	0.0
N5−H61···O9	96.1	89.7	0.0	0.0	0.0	0.0
N2−H14···O18	82.6	91.3	0.0	95.7	0.0	0.0
N4−H44···O6	90.3	96.2	76.1	0.0	6.2	0.0
N6−H74···O12	92.0	81.2	9.8	0.0	0.0	0.0

Table 7. Oxygen Coordination at Various Points on the K^+ PMF Profile through the HyV Face and the Lac Face Minimum

point on profile	carbonyl coord	MeOH coord	total coord
minimum (0.25 Å)	6.0	1.0	7.0
2.5 Å	3.3	3.1	6.4
maximum (4.75 Å)	1.0	4.4	5.4
minimum (6.25 Å)	0.0	5.5	5.5
9.0 Å	0.0	6.3	6.3
Lac minimum (−0.5 Å)	6.0	1.1	7.1

MD trajectories were run at the minimum (0.25 Å), the shoulder (2.5 Å), the maximum (4.75 Å), the second minimum (6.25 Å), and the endpoint (9.0 Å) of the HyV profile and the minimum of the Lac profile (−0.5 Å) for the K^+ simulations. We monitored the percentage of time the intramolecular hydrogen bonds were formed and the oxygen coordination of the ion for each of the various points on the K^+ PMF profile. Table 6 shows this data for the K^+ decomplexation. The criteria we used for the presence of an intramolecular hydrogen bond are an O−H distance of ≤2.6 Å and an N−H−O angle between 120° and 240°. Generally, as the ion is pulled out of the complex, the percentage of time the intramolecular hydrogen bonds exist decreases as would be expected. Table 7 shows the oxygen coordination for the K^+ profiles. Any oxygen within 4.0 Å is considered to be coordinated to the ion. As the ion is pulled out of the ionophore, the carbonyl oxygen coordination decreases while the methanol oxygen coordination increases as would be expected. Comparing the two minima of the K^+ profile in Table 7, we found the carbonyl coordination to be the same, although the methanol coordination differs by 0.1. Representative structures for the HyV face minimum and the Lac face minimum can be found in Figures 8 and 9. Examining Figures 8 and 9, one can see that methanol molecules can penetrate through the face of valinomycin.

Examination of the shoulder indicates that the carbonyl oxygen coordination is approximately 3.3. Graphical analysis of a representative structure at this point (see Figure 10) shows the beginning of the loss of ion coordination by two of the bottom set of carbonyl oxygens and one of the upper set. Hence, the change in the slope of the PMF curves at this point can be mostly ascribed to the loss of several of the bottom three carbonyl−ion interactions.

Examination of the coordination at the maximum reveals that the carbonyl oxygen coordination is approximately 1.0. Graphical analysis of a representative structure at this point (see Figure 11) shows one of the carbonyl oxygens hydrogen bonding with a methanol coordinating the ion. At this point, the ion and ionophore are not quite separated by a solvent layer. There are still some direct carbonyl−ion interactions. This point on the PMF profile will be discussed in greater detail later when this maximum and the Na^+ profile maximum are compared.

Na^+ Results. Figure 12 shows the PMF profile for Na^+ being pulled through the HyV face. The Lac face was not examined

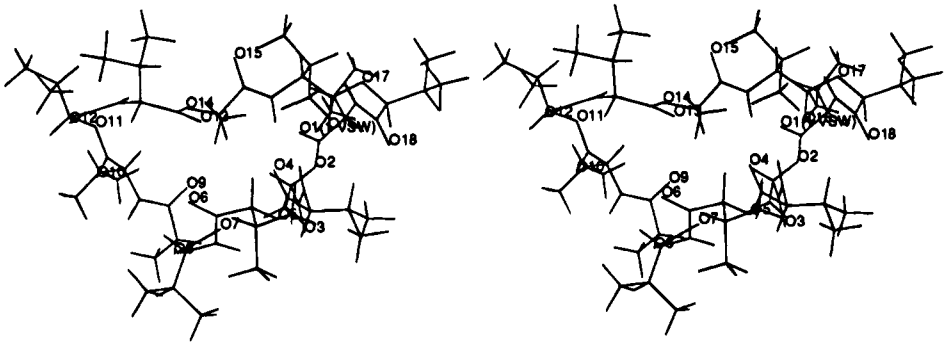

Figure 6. Stereoview of a representative structure of the endpoint (9 Å COM separation) of the K^+−HyV profile.

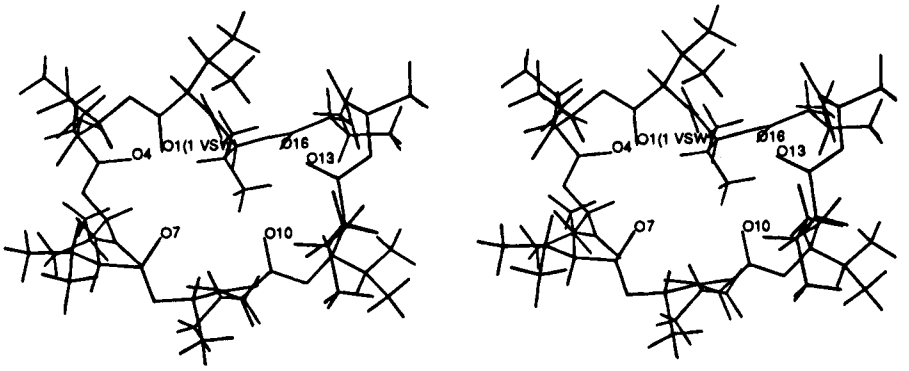

Figure 7. Stereoview of a representative structure of the endpoint (9 Å COM separation) of the K^+−Lac profile.

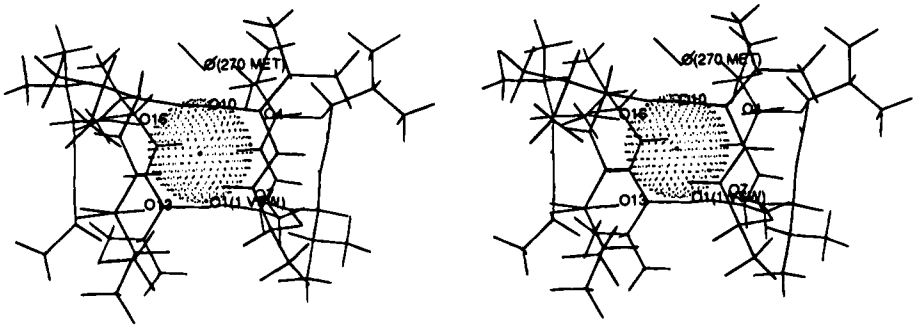

Figure 8. Stereoview of a representative structure at the K^+−HyV face minimum. The top face is the HyV face.

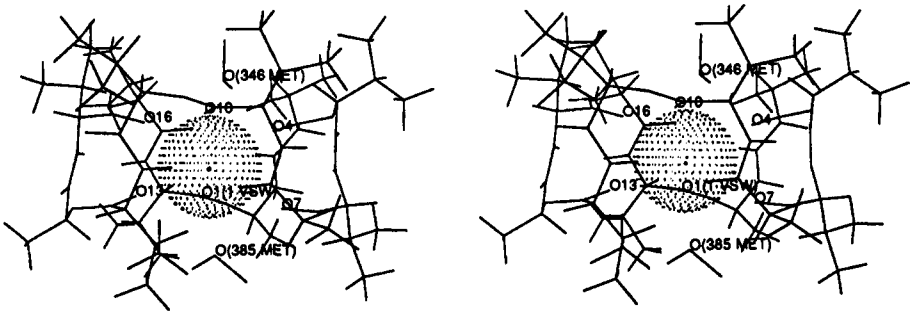

Figure 9. Stereoview of a representative structure at the K^+−Lac face minimum. The top face is the Hyv face.

in this case due to the observation that it had a higher barrier than did the HyV face in the case of K^+. The general shape of the HyV profile is different than the shape of the HyV profile of K^+. The energy steeply rises until ~1.75 Å COM separation, where there is a maximum. From the maximum, a minimum is formed at a COM separation of 2.5 Å. The energy then continues to rise until the ion and the valinomycin molecule share a contact layer of solvent at ~4.75 Å. Then the energy decreases as the Na^+ and valinomycin become further solvent-separated. Integration of the curve to estimate the free energy of association gives 1.1 kcal/mol. This value lies below the experimental value of -1.2 ± 0.4 kcal/mol. Our integrated association constant indicates that Na^+ does not bind to valinomycin. This observation is discussed further in the Discussion section. Figure 13 shows the PMF profiles of Na^+ (solid line) and K^+ (dashed line) through the HyV face where both of the endpoints are arbitrarily set to zero for the sake of comparison of the shape of the profiles. The minimum of the Na^+ profile is slightly broader than the K^+ profile while the barrier to association/dissociation is ~2 kcal/mol higher. Furthermore, the Na^+ profile contains at minimum at ~2.5 Å instead of the shoulder observed in the K^+ profile.

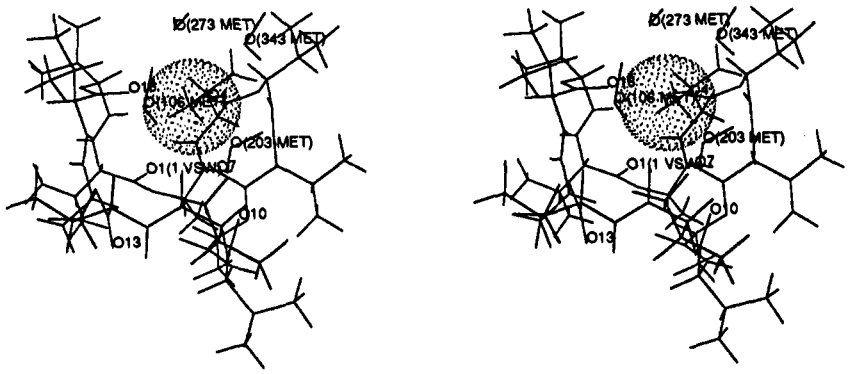

Figure 10. Stereoview of a representative structure at 2.5 Å COM separation on the K^+–HyV face minimum. The top face is the HyV face.

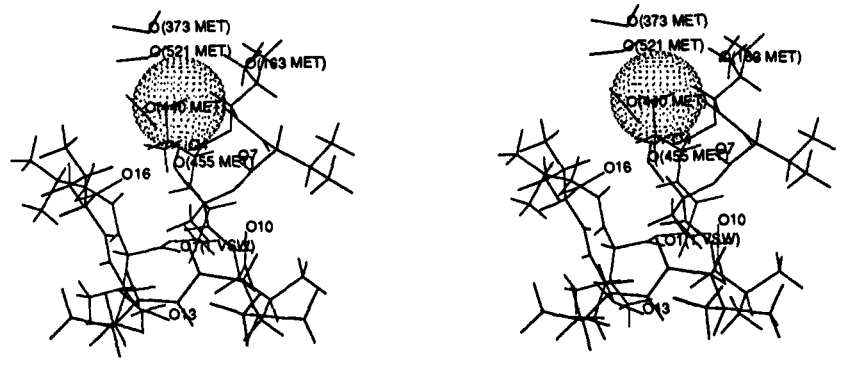

Figure 11. Stereoview of a representative structure at he maximum of the K^+–HyV profile. The top face is the HyV face.

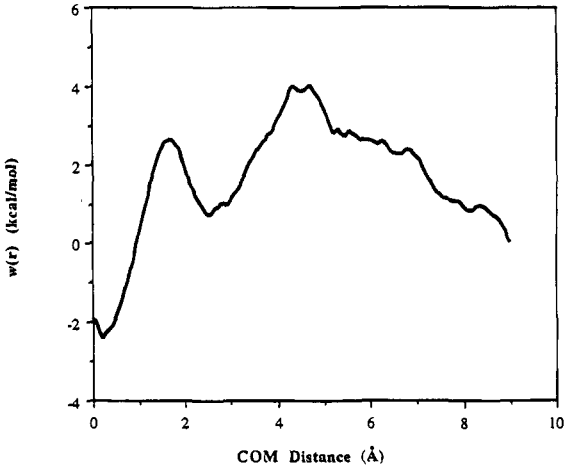

Figure 12. PMF profile for Na^+ being discharged through the HyV face.

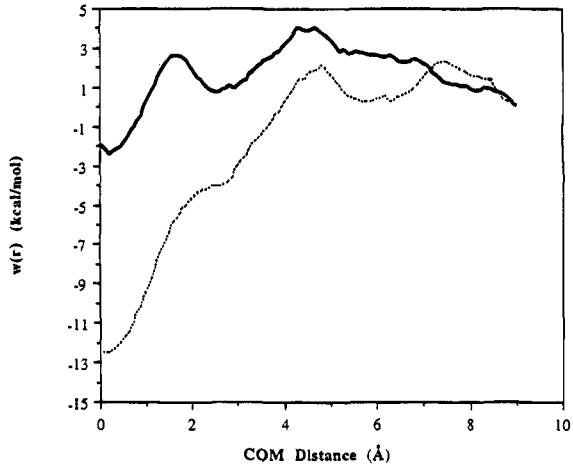

Figure 13. Comparison of the K^+ (dashed line) and Na^+ (solid line) PMF profiles calculated by discharging the ion through the HyV face.

MD trajectories were also run at the minimum (0.25 Å), the first transition state (1.75 Å), the second minimum (2.5 Å), the maximum (4.75 Å), and the two endpoints (6.0 and 9.0 Å) of the HyV face of the Na^+ simulations. We monitored the percentage of time the intramolecular hydrogen bonds were formed and the oxygen coordination of the ion for each of the various points along the Na^+ PMF profiles. Table 8 shows the percentage of time the intramolecular hydrogen bond exists for Na^+ decomplexation. The criteria was used for the presence of an intramolecular hydrogen bond were described in the K^+ simulation results. Generally, as the ion is pulled out of the complex, the percentage of time the intramolecular hydrogen bonds exist decreases as was seen in the K^+ simulation. Comparing the trends for the K^+ (see Table 6) and Na^+ (see Table 8) cases, we find that the intramolecular hydrogen bonds break at a similar COM separation for the Na^+ and the K^+ decomplexation. Table 9 shows the oxygen coordination for Na^+ profiles. Not unexpectedly, the carbonyl oxygen coordination decreases while the methanol oxygen coordination increases as the ion discharges into solvent.

Table 8. Analysis of Percentage of Time the Intramolecular Hydrogen Bonds Exist at Various Points on the Na^+ PMF Profile through the HyV Face

	percentage of time H-bonded (%)					
H bond	minimum (0.25 Å)	1.75 Å	2.5 Å	maximum (4.75 Å)	6.25 Å	9.0 Å
N1–H1···O15	93.8	84.2	93.9	66.8	89.2	78.3
N3–H31···O3	95.9	55.3	85.2	97.3	0.0	0.0
N5–H61···O9	88.9	50.3	89.9	0.0	19.3	0.0
N2–H14···O18	92.7	95.8	96.9	52.9	0.0	0.0
N4–H44···O6	88.9	94.1	94.6	0.0	0.0	0.0
N6–H74···O12	97.2	92.0	98.0	0.0	72.8	54.4

A representative structure of the Na^+ HyV face minimum can be found in Figure 14. The carbonyl coordination is 6.0 (see Table 9), which is identical to what was seen for the K^+

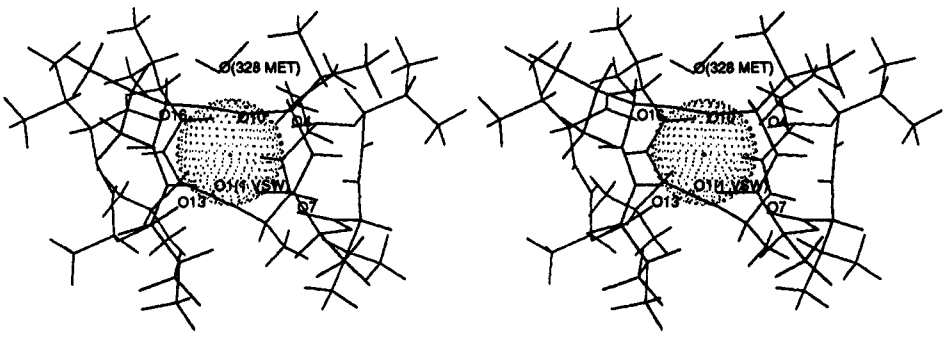

Figure 14. Stereoview of a representative structure at the Na^+−HyV face minimum. The top face is the HyV face.

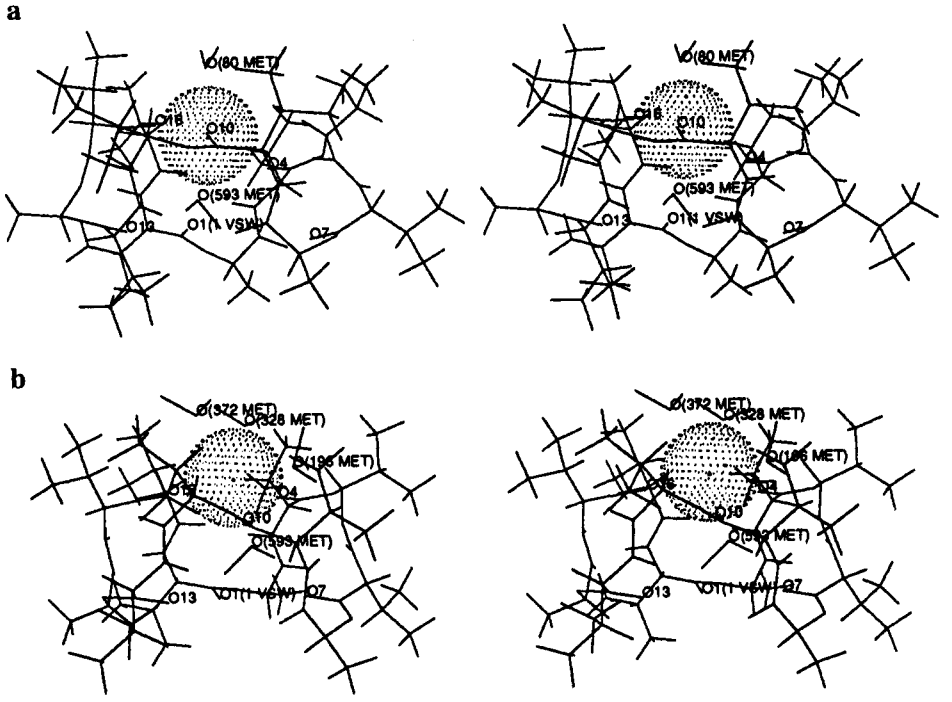

Figure 15. Stereoview of representative structures at (a) 1.75 Å COM and (b) 2.5 Å COM separation on the Na^+−HyV profile. The top face is the HyV face.

Table 9. Oxygen Coordination at Various Points on the Na^+ PMF Profile through the HyV Face

point on profile	carbonyl coord	MeOH coord	total coord
minimum (0.25 Å)	6.0	1.0	7.0
1.75 Å	5.2	2.3	7.5
2.5 Å	3.0	3.1	6.1
maximum (4.75 Å)	0.0	6.0	6.0
6.25 Å	0.0	5.9	5.9
9.0 Å	0.0	5.9	5.9

structures (see Table 7). This minimum is at 0.25 Å, and one methanol penetrates the HyV face of the molecule. Graphical analysis of a representative structure at the first transition state of the Na^+ profile (see Figure 15a) shows the beginning of the loss of ion coordination by the bottom set of three carbonyl oxygens, which was also seen at the shoulder of the K^+ profile. Moreover, a second methanol is interacting with the Na^+ ion through the Lac face of valinomycin. This second methanol molecule also forms a hydrogen bond with one of the bottom carbonyls that are no longer coordinating the Na^+ ion. Finally, the upper carbonyl oxygens form a ring around the Na^+ ion, which brings the total coordination number for this point to ~7.5 (5.2 carbonyl and 2.3 MeOH). At 2.5 Å, a second minimum is formed (see Figure 15b), which still retains the upper carbonyl interactions. However, at this point, two new methanol molecules are able to coordinate to the Na^+ ion through the HyV face of valinomycin. The coordination in this case decreases to ~6.1 as opposed to ~7.5 at the 1.75 Å point. It is interesting that a decrease is observed along the PMF profile on moving from 1.75 to 2.5 Å. This change results in the carbonyl interactions decreasing from 5.3 to 3.0, while the MeOH coordination increases from 2.3 to 3.1. Hence, it appears that the MeOH coordination is highly favored over carbonyl coordination for Na^+. This is discussed further below.

At the maxima of the K^+ and Na^+ curves, the ion and ionophore are not quite separated by a contact layer of solvent for the former, while for the latter they are. This can be seen in Figures 11 and 16, respectively. On average, zero carbonyl oxygens are interacting directly with the Na^+ ion, while 1.0 carbonyl is interacting directly with the K^+ ion (see Tables 7 and 9). It is very difficult to determine the exact point where the ion and ionophore share a solvent layer due to the high conformational flexibility of this region along the profiles. Graphical analysis of the endpoints of the simulations at different COM separations indicates that the ion and ionophore share the same solvent layer at ~0.5 Å past the maximum for the K^+ case.

Discussion

The association of K^+ and Na^+ with valinomycin was examined in methanol using free energy techniques. The charge

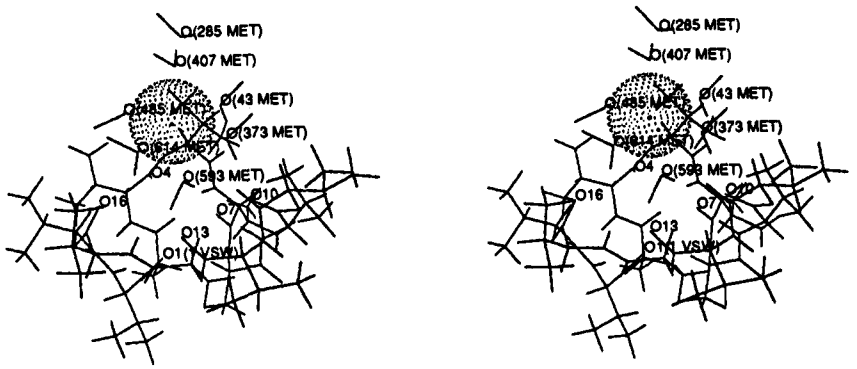

Figure 16. Stereoview of a representative structure at the maximum of the Na^+–HyV profile. The top face is the HyV face.

model that best reproduced the relative free energy of binding of K^+ and Na^+ to valinomycin was determined using semiempirical techniques. Electrostatic potential charges were determined for the propeller crystal structure using the MNDO Hamiltonian in MOPAC 6.0. However, it has been seen that this method of charge determination may give unrealistic charges for buried atoms in the molecule.[51,52] A better method for handling this has been implemented by Kollman and co-workers, and it places constraints on the values of the buried atoms,[51,52] We did not observe this flaw in our charge model, and the point charges obtained for valinomycin reproduced the electrostatic potential of the molecule and have done well in reproducing the free energy of binding of the ions to valinomycin. When computationally feasible, determining the ESP charges for the entire moleucle gives a better representation of the charge distribution in the molecule.[43] Using a residue-based approach, the charges are calculated for each residue and forced to be a unit of charge. In our case, each residue was forced to be neutral so that the entire valinomycin molecule would be neutral when utilizing the residue-based approach. Although forcing the residue to be neutral is a reasonable assumption, it is possible that the residue carries a fraction of charge in the molecule. Thus, determining the charges for the entire molecule is a better approach compared to the residue-based approach when the size of the molecule permits execution of the calculation.

We find that valinomycin prefers to bind Na^+ by -12.9 kcal/mol (see Table 5). This difference is less than the preference observed for the two ions in MeOH ($K^+ \rightarrow Na^+$ is -17.4 kcal/mol). Thus, the carbonyl contacts made by Na^+ with valinomycin are not of sufficient strength to overcome the stabilization afforded Na^+ in MeOH. On the other hand, K^+ makes contacts of sufficient strength in the VK^+ complex, which results in the complex being stabilized relative to the free ion and ionophore. Cs^+ is much larger than K^+, and yet it lies between K^+ and Na^+ in the selectivity sequence. Perhaps valinomycin is capable of binding Cs^+, but the intramolecular hydrogen bonding is destabilized due to elongation of the hydrogen bonds in order to fit the larger ion into the cage. This would destabilize the Cs^+ complex relative to the K^+ and result in the observed selectivity ordering.

Rate constants for the association and dissociation processes can be calculated from the barrier heights determined from the PMF profiles. The barriers to association are 4.0 and 2.3 kcal/mol for Na^+ and K^+, respectively. The barriers to disassociation are 6.5 and 14.8 kcal/mol for Na^+ and K^+, respectively. These barrier heights can be converted using standard techniques.[53] Comparison of the calculated rate constants to experimental kinetic data can be found in Table 10. The experimental data were obtained at 25 °C for valinomycin in methanol. The rate constant for K^+ was determined in the presence of tetramethylammonium perchlorate. Although the K^+ rate constants were determined under slightly different conditions than the Na^+ rate constants, the data can be compared to the calculated rate constants to provide insight into the effectiveness of our valinomycin model to reproduce kinetic data. The rate constant that we calculated for the association of Na^+ with valinomycin is too low when compared (ΔG_{on} (calcd) = 4.0 kcal/mol *vs* ΔG_{on} (exp) = 7.7 kcal/mol) with the experimental value. On the other hand, the calculated dissociation rate constant was found to be in better accord with the experimental value (ΔG_{off} (calcd) = 6.5 kcal/mol *vs* ΔG_{off} (exp) = 8.9 kcal/mol), but it was still too low. From the experimental and calculated on and off rates we can estimate the free energy of binding of Na^+ to valinomycin to be -1.2 kcal/mol (exp) and -2.5 kcal/mol (calcd). The agreement of the theoretical free energy of binding calculated using the on and off rate constants is better than that obtained *via* integrating the free energy profile (~1.1 kcal/mol). The calculated rate constants for K^+ overestimate the rate constant for association (ΔG_{on} (calcd) = 2.3 kcal/mol *vs* ΔG_{on} (exp) = 7.1 kcal/mol) and slightly underestimate the rate constant for dissociation (ΔG_{off} (calcd) = 13.2 kcal/mol *vs* ΔG_{off} (exp) = 14.8 kcal/mol). This is consistent with the tight binding of the K^+ ion seen with our model. Using the calculated rate constants, we estimate that the free energy of binding of K^+ to valinomycin is -12.5 kcal/mol, which is roughly twice as large as the experimental value of -6.4 ± 0.4 kcal/mol and the integrated value of -7.4 kcal/mol.

Table 10. Comparison of the Barrier Heights of the K^+ and Na^+ PMF Profiles with Experimental Kinetic Data for the Binding of Ions to Valinomycin in MeOH at 25 °C

ion	k_{on} (M^{-1} s^{-1})	ΔG_{on} (kcal/mol)	k_{off} (s^{-1}1)	ΔG_{off} (kcal/mol)	ΔG_{bind} (kcal/mol)
		Experimental Data[a]			
Na^+	1.4×10^7	7.7	2×10^6	8.9	−1.2
K^+	4×10^7	7.1	1.3×10^3	13.2	−6.1
		Obtained from PMF Profiles			
Na^+	7.3×10^9	4.0	1.1×10^8	6.5	−2.5
K^+	1.3×10^{11}	2.3	8.5×10^1	14.8	−12.5

[a] Taken from ref 5. The potassium values were determined in 0.1 M tetramethylammonium perchlorate.

(51) Bayly, C. I.; Cieplak, P.; Cornell, W.; Kollman, P. A. A Well-Behaved Electrostatic Potential Based Method Using Charge Restraints for Deriving Atomic Charges: The RESP Model. *J. Phys. Chem.* **1993**, *97*, 10269–10280.

(52) Cornell, W. D.; Cieplak, P.; Bayly, C. I.; Kollman, P. A. Application of RESP Charges to Calculate Conformational Energies, Hydrogen Bond Energies, and Free Energies of Solvation. *J. Am. Chem. Soc.* **1993**, *115*, 9620–9631.

(53) Alberty, R. A.; Daniels, F. *Physical Chemistry*, 5th ed.; John Wiley & Sons: New York, 1979.

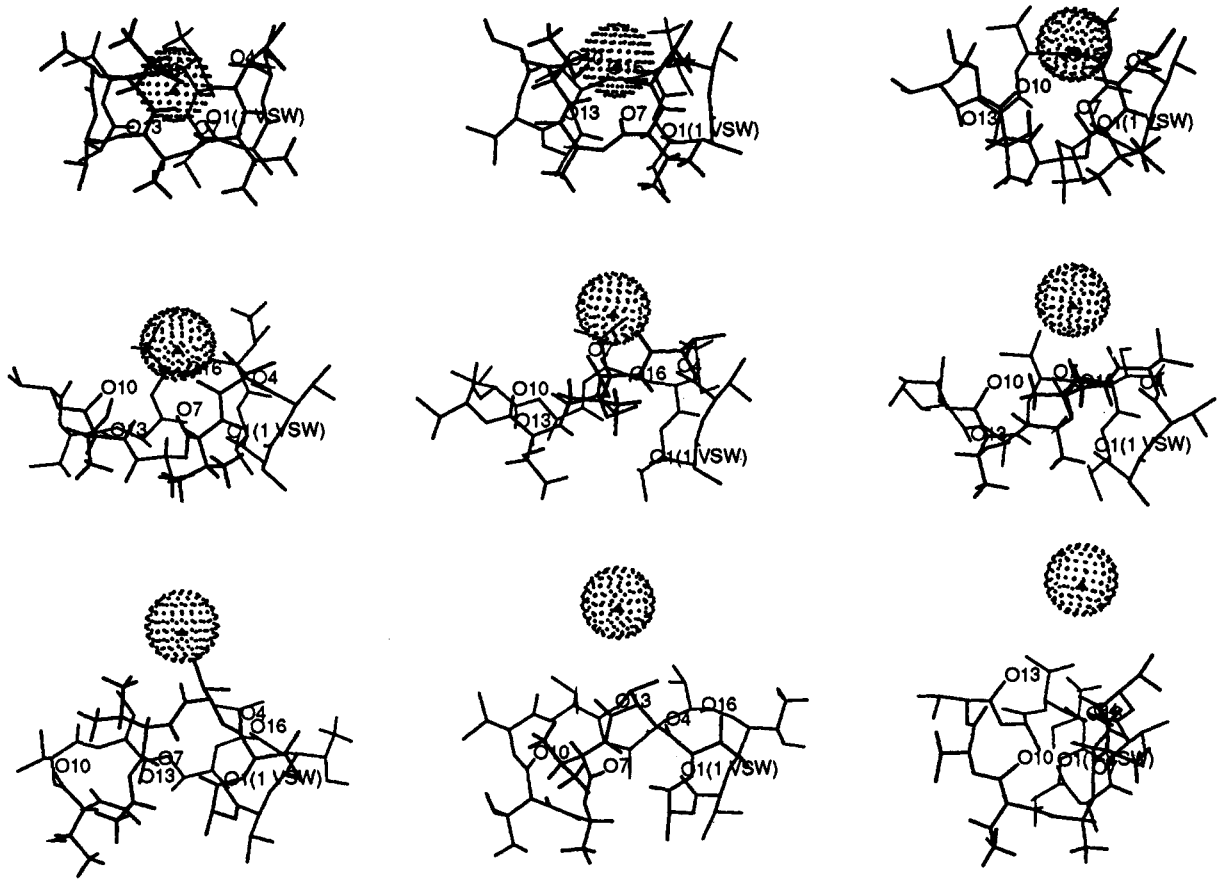

Figure 17. Representative structures along the K^+–HyV PMF profile. The COM separation distances are 1, 2, 3, 4, 5, 6, 7, 8, and 9 Å, respectively, viewing the figure from the top to bottom/left to right. Hydrogens are omitted for clarity. The top face is the HyV face.

The calculated range of free energies of binding of K^+ to valinomycin overestimated the average experimental free energy of binding[7] by ~1–6.1 kcal/mol, while the calculated range of free energies of binding of Na^+ staggered the experimental free energy of binding.[7] One possible source of error is that the path directly through the faces of the molecule is not the lowest energy path. To determine this would require relaxing some of the constraints we have employed (especially removal of the COM rotation). However, this greatly increases the conformational complexity of this already complicated problem because many more potential minima need to be sampled. Also, the integration used to determine the K_a value was derived for the association of spherical (or hemispherical) objects. Since valinomycin is not a sphere or hemisphere, the K_a obtained in this way is only an approximation and not a rigorously derived value.

We find that the endpoint regions of the profiles have not leveled off completely, which introduces an error in the placement of the zero point of the profile. Thus, the calculated on rate constants are subject to much higher uncertainty than are the off rate constants, and indeed, we find that the latter are in better accord with experimental values than are the former. Hence, determination of the association constant using the k_{on}/k_{off} ratio will suffer from the relatively larger inaccuracies in k_{on} relative to k_{off}. Perhaps, better convergence near the maximum and beyond could be obtained using longer periods of time and increasing the number of simulations in the area.[54,55] However, to sample all possible conformations will require very extensive simulations as has been pointed out by Straatsma and McCammon[55] and Sun and Kollman[54] in the case of 18-crown-6. Nevertheless, this may then improve the kinetic and thermodynamic data obtained from these models. Although the valinomycin and ion models were not effective at quantitatively reproducing experimental kinetic data, the models reproduced the trends in the kinetic data. The models predict that the rate of dissociation for Na^+ is greater than K^+ and the rate of association for K^+ is greater than Na^+. Finally, it should be stressed that determining a K_a for a complex association process is very difficult due to a number of factors (*e.g.* potential function errors, sampling errors, *etc.*).

The difference in the difficulty of desolvation of K^+ and Na^+ is reflected in their barrier heights to association. Na^+ is better solvated in methanol than K^+ by ~17 kcal/mol, which makes it energetically more difficult to strip solvent from the first coordination shell of Na^+. The solvent must be stripped from the ion so it can bind with the valinomycin carbonyl oxygens. Thus, the barrier to association should be higher for Na^+ than K^+, because the process of removing solvent from Na^+ requires more energy. The barrier heights calculated from our simulations reflect this trend.

Figures 17 and 18 show the association of K^+ and Na^+, respectively. Both association processes take place in a similar manner. The top three carbonyls strip methanols from the first coordination shell of the ion and then coordinate the ion. As the ion to ionophore COM decreases, the intramolecular hydrogen bonds form and the ion becomes ligated by the bottom carbonyls. This visual analysis shows the valinomycin complex

(54) Sun, Y.; Kollman, P. A. Molecular Dynamics Simulations: 18-Crown-6 as a Test Case. *J. Comput. Chem.* **1992**, *13*, 33–40.

(55) Straatsma, T. P.; McCammon, J. A. Treatment of Rotational Isomers in Free Energy Calculations. II. Molecular Dynamics Simulation Study of 18-Crown-6 in Aqueous Solution as an Example of Systems with Large Numbers of Rotational Isomeric States. *J. Chem. Phys.* **1989**, *91*, 3631–3637.

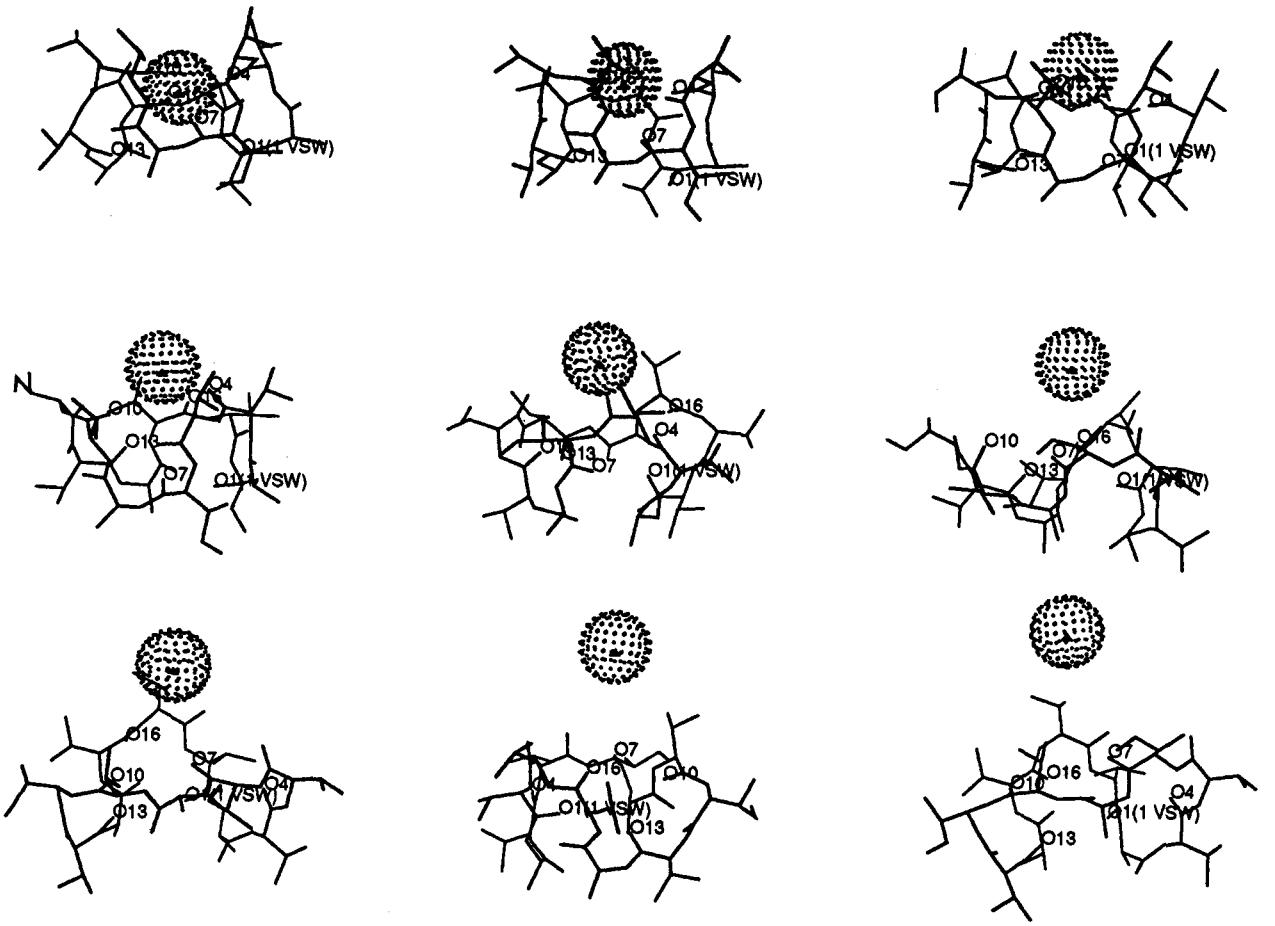

Figure 18. Representative structures along the Na^+–HyV PMF profile. The COM separation distances are 1, 2, 3, 4, 5, 6, 7, 8, and 9 Å, respectively, viewing the figure from the top to bottom/left to right. Hydrogens are omitted for clarity. The top face is the HyV face.

to be more conformationally flexible for the association with K^+ than Na^+. The binding of the ion induces rigidity in the molecule because of the intramolecular hydrogen bonding and close ion–carbonyl contacts that occur during the association. This induced rigidity then results in the final formation of the ion/ionophore complex.

Although ion discharge through the HyV and Lac faces must be thermodynamically equivalent, they do not necessarily need to be kinetically equivalent. In higher polarity solvents where the propeller type structure is found, discharge through the HyV face could be kinetically favored over the Lac face, because the Lac face would need to rearrange with respect to the propeller after the discharge of the ion. The propeller crystal structure (Figure 1) shows the methyl groups of the Lac residues inside the propeller. As the ion is discharged through the HyV face, the three "flaps" of the molecule fold down to form the propeller and force the methyl groups into the center of the molecule. Discharging the ion through the Lac face would force isopropyl groups into the center of the molecule, which would be more sterically unfavorable. Thus, our results suggest ion discharge would be favored through the HyV face in polar solvents. This also explains why the Lac face endpoint is higher in energy than the HyV endpoint (see Figure 5). The Lac face cannot directly convert to the propeller structure since it requires extensive molecular reorganization. Given the short periods of time used in our PMF simulation, the final Lac face structures are unable to rearrange into the lower energy HyV face structures and, hence, the Lac and HyV endpoint structures are not at the same energy value.

We can speculate as to how valinomycin may transport an ion through a membrane based on our theoretical results. Experimental kinetic data show that the on and off rates for transport of K^+ through a phosphatidylinositol bilayer are equal.[5] This suggests that both faces are kinetically equivalent or the unloading and loading of the ion takes place through the same face. Provided both faces are kinetically equivalent, the ion could bind or discharge through either the Lac face or the HyV face. However, there are two possible methods of transportation across the membrane if the ion is loaded and discharged through the same face. If the uncomplexed form of valinomycin that sits at the surface of the membrane resembles the crystal structure in Figure 2 (the crystal structure determined in octane), it is possible that the ion binds through the Lac face (isopropyl, methyl) while the more "greasy" HyV face is buried in the bilayer. The ionophore could tumble as it transports the ion through the bilayer. Valinomycin could then release the ion from the Lac face while keeping the HyV face buried. On the basis of our data in methanol, we have suggested that it would be faster to discharge the ion through the HyV face in a polar environment. If the uncomplexed form of valinomycin that sits at the surface of the membrane resembles the propeller, loading and discharge of the ion may occur through the HyV face. As the propeller binds the ion through the HyV face, the complex would project the HyV face into solution. The unfavorable interactions of the isopropyl groups with the aqueous solution could be a force to drive the isopropyl groups into the bilayer and begin ion transport. Once in the bilayer, it is conceivable that the valinomycin complex could rotate and discharge the ion into solution. During discharge, the unfavorable interactions between the isopropyl groups of the HyV face and the solution could be a driving force for quick release of the ion and return

to a propeller state. Our data support the latter supposition if there is indeed a facial selectivity.

Not only does this study provide insight into the association process of valinomycin, but it also provides insight into free energy techniques and model development. The valinomycin model used in this study reproduces the relative and absolute free energies of binding of K^+ and Na^+ reasonably well. The PMF calculations provide a more stringent test of a model than relative free energy determinations, but it is more difficult to model due to the conformational flexibility of valinomycin. It is possible for a model to consistently overestimate or underestimate the absolute free energies of association and reproduce the relative free energies of binding only and give no indication of absolute errors in the model.[56,57] Thus, PMF profiles not only provide energetic and structural information about the association process of ions with ionophores, but they also provide a test of the validity of the ionophore and ion models.

(56) Åqvist, J. Ion–Water Interaction Potentials Derived from Free Energy Perturbation Simulations. *J. Phys. Chem.* **1990**, *94*, 8021.

(57) Marrone, T. J.; Merz, K. M., Jr. Transferability of Ion Models. *J. Phys. Chem.* **1993**, *97*, 6524–6529.

Conclusions

In this study we have used free energy perturbation studies to examine the association process of K^+ and Na^+ with the ionophore valinomycin. The relative free energies are in good agreement with experimental values, and the calculated ranges for the absolute free energies of binding are found to be in reasonable accord with experimental values for Na^+ and are overestimated for K^+. The origin of the high preference for K^+ over Na^+ appears to be due to the inability of valinomycin to overcome the solvation free energy of Na^+ in MeOH through effective ion–carbonyl contacts within the ionophore. Finally, we have presented mechanisms by which valinomycin carries out its ion transport function.

Acknowledgment. This research was supported by the ONR (N00014-90-3-4002) and ACS-PRF (23225-G6,4). We also thank the Pittsburgh Supercomputer Center for CRAY YMP time and the Center for Academic Computing for IBM 3090 time.

JA931384E